Stress-induced nematicity in EuFe$_2$As$_2$ studied by Raman spectroscopy

W.-L. Zhang,[1,2,*] Athena S. Sefat,[3] H. Ding,[1,4] P. Richard,[1,4] and G. Blumberg[2,5,†]

[1]*Beijing National Laboratory for Condensed Matter Physics and Institute of Physics, Chinese Academy of Sciences, Beijing 100190, China*
[2]*Department of Physics and Astronomy, Rutgers University, Piscataway, New Jersey 08854, USA*
[3]*Materials Science and Technology Division, Oak Ridge National Laboratory, Oak Ridge, Tennessee 37831-6114, USA*
[4]*Collaborative Innovation Center of Quantum Matter, Beijing, China*
[5]*National Institute of Chemical Physics and Biophysics, Akadeemia tee 23, 12618 Tallinn, Estonia*

We use polarized Raman scattering to study the structural phase transition in EuFe$_2$As$_2$, the parent compound of the 122-ferropnictide superconductors. The in-plane lattice anisotropy is characterized by measurements of the side surface with different strains induced by different preparation methods. We show that while a fine surface polishing leaves the samples free of residual internal strain, in which case the onset of the C_4 symmetry breaking is observed at the nominal structural phase transition temperature T_S, cutting the side surface induces a permanent fourfold rotational symmetry breaking spanning tens of degrees above T_S.

The 122-ferropnictide superconductors go through a structural phase transition at a temperature T_S that coincides with or precedes a magnetic phase transition at a temperature T_N [1]. In most of the parent and underdoped ferropnictides, measurements of electronic anisotropy are reported below T_S [2–5]. Above T_S, unexpected anisotropy is found to be persistent in experiments performed under uniaxial strain [2,6–8] or magnetic field [9], which implies a nematic phase transition at a temperature $T^* > T_S$. However, other spectroscopic methods claim the absence of such nematic transition. Instead, dynamic nematic fluctuations are already present at room temperature and accumulate gradually upon cooling [10–19]. By removing twin domains, uniaxial strain breaks the fourfold rotational symmetry C_4 [20], transforming the structural phase transition into a crossover spanning a measurable temperature range above T_S [21,22]. Consequently, the nematic phase transition above T_S is not universally accepted.

In this paper we study the temperature evolution of stress-induced nematicity above and below the structural phase transition in EuFe$_2$As$_2$, the parent compound of the 122-ferropnictide superconductors. We observe the splitting of the doubly degenerate Fe-As in-plane displacement phonon mode when the lattice C_4 symmetry is broken. We measure this splitting below the structural transition temperature and demonstrate that the splitting is directly proportional to the lattice nematic order parameter. We show that stress occurring during the sample preparation induces permanent C_4-symmetry breaking strain fields that are distinct from dynamic nematic fluctuations above the tetragonal to orthorhombic structural transition.

The EuFe$_2$As$_2$ single crystals (with $T_S = 175$ K) used in this Raman study were synthesized by a Fe-As flux method [23]. We performed Raman scattering from the ac surface prepared by a razor blade cut or fine sandpaper polishing at room temperature. The mechanical polishing has been performed with aluminum oxide sandpapers of several sizes down to 0.1 μm. We used high purity methanol as lubricant. For each

sandpaper, the polished thickness on the sample was precisely controlled to be more than three times the grit size. To minimize strain, we used wax to glue the sample and the adhering point was far away from the measured surface.

We performed the Raman measurements in a quasi-back-scattering optical setup. The 647- and 752-nm wavelength Kr$^+$ laser beams were focused to a $50 \times 100-\mu$m spot on the ac surface of the EuFe$_2$As$_2$ samples. The incident laser power was kept smaller than 10 mW with an estimated 5 K for the laser heating. The laser heating was further verified by the appearance of bright stripes on the ab surface at T_S [16,24] using the same incident power. Temperature-dependent measurements from 30 to 300 K were preformed in a He gas cooled cryostat. The Raman signal was collected and analyzed by a triple spectrometer and a liquid N$_2$ cooled CCD. The Raman susceptibility $\chi''(\omega)$ was calculated using $I(\omega)=[1 + n(T)]\chi''(\omega)$, where $I(\omega)$ is the scattering intensity corrected for the system background and the system optical response, and $n(T)$ is the Bose factor.

The crystal structure of the 122 ferropnictides in the high-temperature tetragonal phase belongs to space group $I4/mmm$ (point group D_{4h}). The corresponding energy and atomic displacements of the Raman active phonons ($1A_{1g} + 1B_{1g} + 2E_g$) at room temperature have been reported previously [25]. Below T_S the crystal structure belongs to space group $Fmmm$ (point group D_{2h}) and the breakdown of the C_4 symmetry splits the degenerate E_g mode into B_{2g} and B_{3g}. In the four-Fe unit cell basis (X-Y coordinates shown in Fig. 1, which is rotated for 45 deg from the two-Fe unit-cell basis), the Raman tensor of the E_g symmetry in the high-temperature phase and that of the B_{2g} and B_{3g} symmetries in the low-temperature phase are [26]

$$R_{E_g} = \begin{pmatrix} 0 & 0 & e \\ 0 & 0 & e \\ e & e & 0 \end{pmatrix}, \quad R_{E_g} = \begin{pmatrix} 0 & 0 & -e \\ 0 & 0 & e \\ -e & e & 0 \end{pmatrix},$$

$$R_{B_{2g}} = \begin{pmatrix} 0 & 0 & e' \\ 0 & 0 & 0 \\ e' & 0 & 0 \end{pmatrix}, \quad R_{B_{3g}} = \begin{pmatrix} 0 & 0 & 0 \\ 0 & 0 & f' \\ 0 & f' & 0 \end{pmatrix}.$$

*wlzhang@iphy.ac.cn
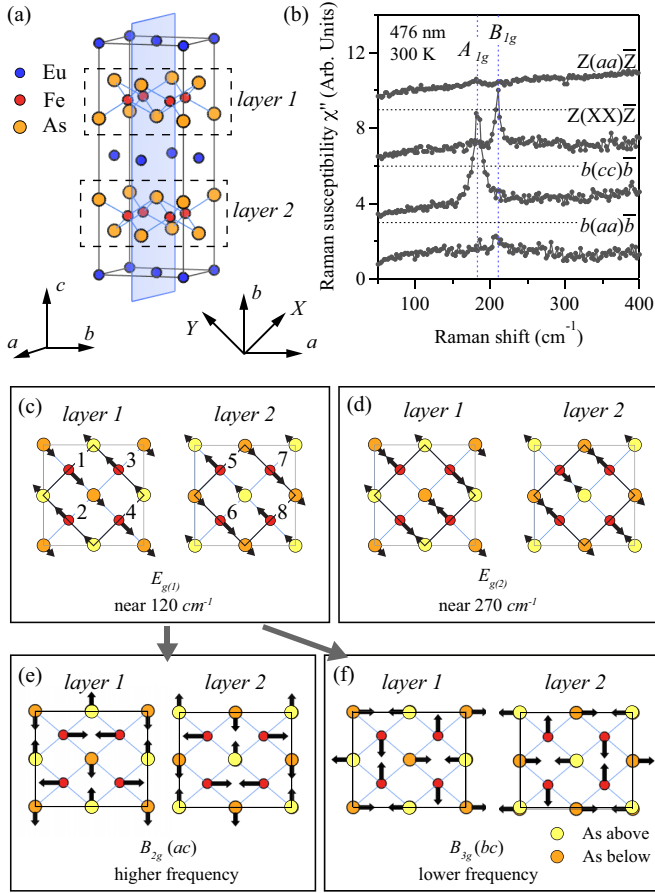†girsh@physics.rutgers.edu

FIG. 1. (a) The orientation of the measured surface (blue rectangle) and the definition of the axis. The light polarization c is defined along the longest axis of the crystal and the polarizations a and b are the longer and shorter nearest Fe-Fe directions, respectively. The X and Y axes are at 45 deg from a and b. (b) Raman susceptibility χ'' from the side surface and the ab surface. (c) and (d) Atomic displacements of the two E_g modes in the high-temperature tetragonal phase. (e) and (f) Atomic displacements of the B_{2g} and B_{3g} phonons in the low-temperature phase derived from the lower-energy branch of the two degenerate E_g phonons in the high-temperature phase shown in (c).

For the 122 family of iron pnictides, with the body centered lattice, in the high-temperature phase, the long-wavelength lattice displacement at the Brillouin-zone center Γ point are defined by the translational basis vectors of the primitive cell, which require the Fe ion labeled with 1 (Fe-1) to be in phase with Fe-4, Fe-6, and Fe-7 [Fig. 1(c)]. Similarly, Fe-2, Fe-3, Fe-5, and Fe-8 are in phase. For $E_g(B_{2g}/B_{3g})$ symmetry, Fe-1 and Fe-5 are antiphase as required by the horizontal mirror operation (σ_h). Hence, Fe-1 and Fe-2 vibrate in antiphase. The same applies for the As sites. In Figs. 1(c) and 1(d) we illustrate the atomic displacements of the two E_g phonons in the high-temperature phase [Figs. 1(c) and 1(d)] and B_{2g} and B_{3g} phonons derived from the lower-energy branch in the low-temperature phase [Figs. 1(e) and 1(f)]. Our analysis is consistent with Refs. [22,27]. Here we only consider the symmetry operations, whereas the relative length of the arrows

on the Fe and As do not contain information on the vibration amplitude.

The B_{2g} mode is active for ac polarization, whereas the B_{3g} mode is active for bc polarization. Unlike many other symmetry-sensitive probes that require external uniaxial field to eliminate the average effect from twin domains, the B_{2g} and B_{3g} modes can both be detected when there are naturally formed twin domains, which allows the measurement of the lattice anisotropy in a free standing sample.

The orientation of the side surface we obtain is shown by the blue rectangle in Fig. 1(a). We further justify it by selection rules of the B_{1g} phonon for different polarization configurations. According to the selection rules, $I_{XX} = A_{1g} + B_{1g}$, $I_{aa} = A_{1g} + B_{2g}$, and $I_{cc} = A_{1g}$. In Fig. 1(b) we show the spectra: aa polarization configurations measured from the ab surface, XX measured from the ab surface, cc measured from the side surface, and parallel polarizations in the ab plane measured from the side surface from top to bottom. In the last spectrum, the B_{1g} phonon is absent, which indicates that the polarization configuration is aa, instead of XX. This confirms that the measured surface is the ac surface.

Figure 2(a) shows Raman spectra measured with cross polarizations (ac) at room temperature. From a surface obtained by razor blade cut (blue curve), the spectra show six peaks between 18 and 220 cm^{-1}. The peak around 120 cm^{-1} is the lower-energy branch of the E_g mode [28]. The three sharp peaks at 19.4, 29.2, and 95.4 cm^{-1} marked with stars are the laser plasma lines. By comparison with previous phonon measurements on the 122-ferropnictide materials [25], we assign the two modes at 183 and 214 cm^{-1} marked with pound signs to the A_{1g} and B_{1g} phonons, respectively. These two modes should only be Raman active for the in-plane and ZZ polarization configurations. The observation of A_{1g} and B_{1g} phonons in the ac polarization configuration suggests the measured surface is bent or contains fragment pieces induced by the cut with the razor blade.

In order to improve the surface quality, we polished the cutting surface to optical flatness [Fig. 2(e)]. From the polished surface (red curve), the scattering background and the laser plasma lines are greatly suppressed. The Raman scattering signals from other symmetry channels are also removed.

In Figs. 2(b) and 2(c) we show Raman spectra measured with ac polarization from the two surfaces at different temperatures above and below T_S. A clear splitting of the E_g mode is observed below 175 K.

In order to extract further information about the structural transition, we fit the E_g mode for $T > T_S$ using a single Lorentz function and a linear background:

$$\chi''_{ac}(\omega,T) = \mathrm{Lor}(\omega,\omega_0,\gamma_0,A_0) + a\omega + b, \quad (1)$$

while for $T \leqslant T_S$ we add another Lorentz term to account for the splitting of E_g into $B_{2g} + B_{3g}$:

$$\chi''_{ac}(\omega,T) = \mathrm{Lor}(\omega,\omega_1,\gamma_1,A_1)$$
$$+ \mathrm{Lor}(\omega,\omega_2,\gamma_2,A_2) + a\omega + b. \quad (2)$$

In these expressions $\mathrm{Lor}(\omega,\omega_i,\gamma_i,A_i) = A_i[(\omega - \omega_i)^2 + \gamma_i^2]^{-1}$ is the phonon response, ω_i is the central energy, γ_i is the phonon damping, and $a\omega + b$ is a linear approximation of the background. The fitting curves are displayed in Fig. 2 and
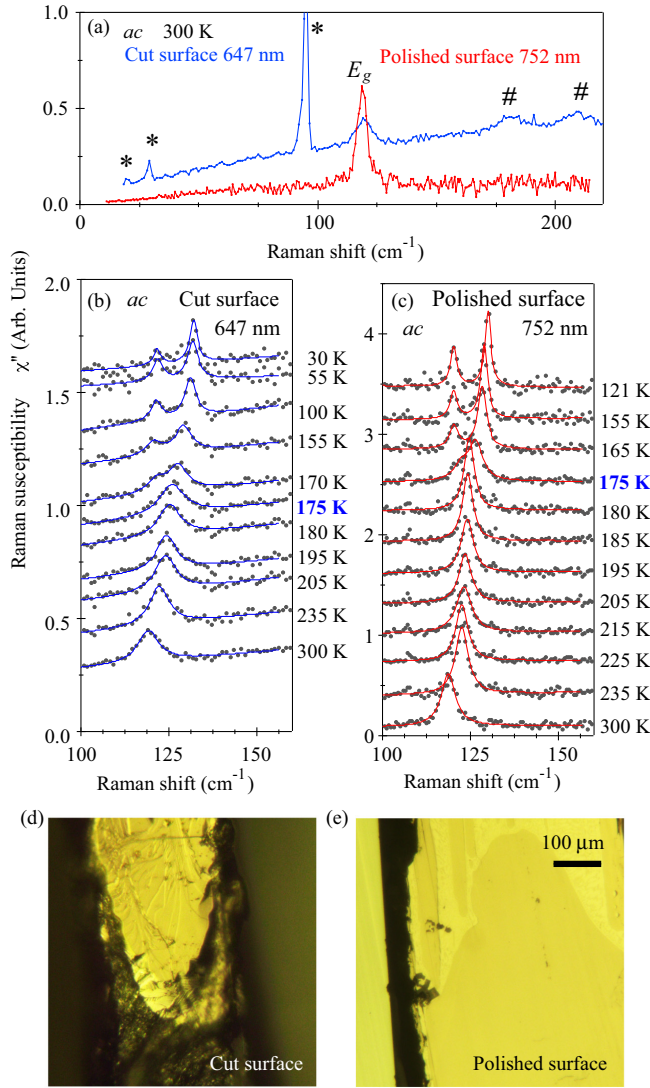
FIG. 2. (a) Raman susceptibility measured with the *ac* polarization configuration at different temperatures on a surface made by a razor blade cut (blue curve) and a surface made by sandpaper polishing (red curve). The three peaks at 19.4, 29.2, and 95.4 cm^{-1} marked with stars are laser plasma lines. The two peaks at 181 and 208 cm^{-1} marked with pound signs are the A_{1g} and B_{1g} phonon modes. (b) and (c) Temperature- dependent phonon spectra measured with the *ac* polarization. The blue and red curves are the fits to Lorentz functions. (d) and (e) Microscopic images of the cut surface and the polished surface, respectively. The reference for the space scaling of the images is given in (e).

the parameters obtained from the fits are plotted in Fig. 3. The energy of the E_g phonon, as well as its B_{2g} and B_{3g} components in the low-temperature phase, are almost identical for the two differently treated surfaces [Fig. 3(a)]. As shown in Fig. 3(b), the phonon energy anisotropy $\frac{\omega_1-\omega_2}{\omega_1+\omega_2}$ can be linearly scaled with the lattice orthorhombic order parameter $\frac{a-b}{a+b}$ in the low-temperature phase [29].

Unlike the phonon energies, the phonon linewidths are strongly dependent on the surface measured. The linewidth of the cut surface γ_{cut} has an overall broadening of about 1.1 cm^{-1} compared to the linewidth of the polished surface
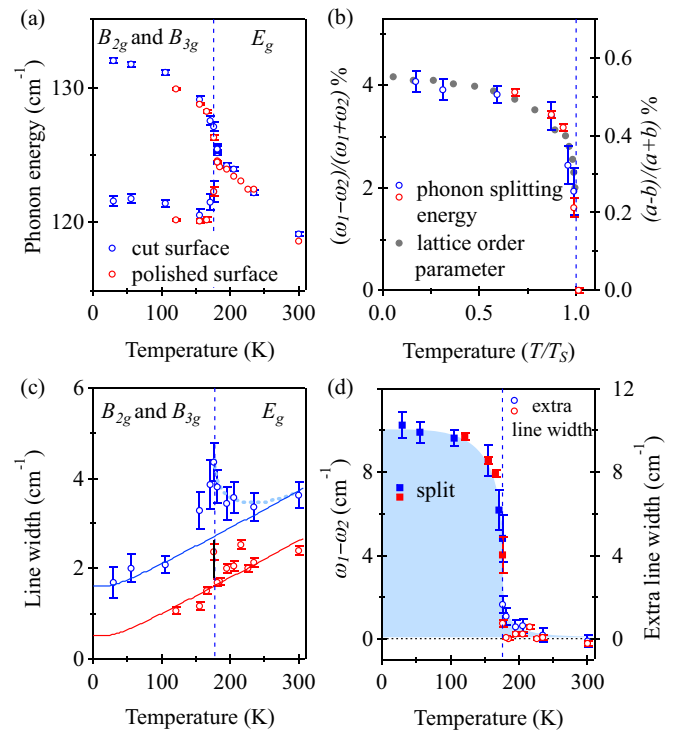

FIG. 3. (a) Phonon energy from the cut surface (blue) and polished surface (red) by fitting to the Lorentz function using Eqs. (1) and (2) above and below T_S, respectively. The dashed vertical line indicates T_S. (b) Phonon energy anisotropy and lattice anisotropy order parameter as a function of temperature. The temperature is scaled by T_S. (c) Phonon linewidth from the two different surfaces. The solid curves are guide lines to the eye. (d) Comparison of the E_g mode extra broadening and B_{2g}/B_{3g} mode splitting for the two surfaces. The vertical error bars are from the fitting error. The temperature error is ±5 K.

γ_{polished} [Fig. 3(c)]. We attribute the overall broadening to the inhomogeneity of the cut surface. Surprisingly, while the decrease of γ_{polished} can be fitted with the expression of the anharmonic decay [30],

$$\gamma_{ph}(T) = \Gamma_0 + \Gamma_1\left(1 + \frac{2}{e^{\hbar\omega_0/2k_BT} - 1}\right), \qquad (3)$$

with $\omega_0 = 129.2 \pm 0.6$ cm^{-1} obtained from ω_{polished} in the high-temperature phase, $\Gamma_0 = 0.1 \pm 0.3$ cm^{-1}, and $\Gamma_1 = 0.4 \pm 0.1$ cm^{-1}, γ_{cut} shows an unusual extra broadening near T_S. The smallest linewidth from the cut surface in the high-temperature phase is at 235 K, which is 60 K above T_S. Interestingly, a similar linewidth broadening is also reported in the E_g mode and the (0,2,0) or (2,0,0) Bragg peaks in BaFe$_2$As$_2$ under uniaxial strain [22,31]. Here we stress that the absence of extra broadening for the E_g mode in the polished sample indicates that the nematic fluctuations are frozen or negligible above T_S, in contrast to previous reports [2,6–9]. As a corollary, the extra broadening in the cut sample thus suggests that the C_4 symmetry is broken above T_S by internal strain rather than by intrinsic dynamic nematic fluctuations. In addition, the difference in the behaviors observed for the two

samples reveals the sensitivity of the Fe-based superconductors to sample preparation.

Since the B_{2g} and B_{3g} phonons cannot be distinguished individually, we conjecture that (1) the strain-induced anisotropy is small compared to the linewidth and the energy resolution and (2) the distribution of the strain is inhomogeneous and it results in a continuous energy splitting. Above T_S the B_{2g} and B_{3g} phonon splitting energy can be approximated by the extra linewidth broadening. In Fig. 3(d) we compare the E_g mode broadening (above T_S) and the B_{2g}/B_{3g} splitting (below T_S) from the two different surfaces. Our results from the cut sample indicate that the structural phase transition changes into a crossover spanning tens of Kelvin above the nominal T_S, which is consistent with other measurements that report nematicity onsets above T_S [2,5–7]. However, the temperature evolution of the order parameter for the second-order phase transition in the polished sample, for which the introduction of strain or stress has been minimized, shows absence of nematic distortion above Ts.

In summary, we reported a Raman scattering study of the in-plane lattice dynamics of EuFe$_2$As$_2$ with two different treatments of the sample side surface (*ac*): the razor blade cut surface that induces residual stress and the fine polished surface for which the internal strain field is minimized. We observed that the energy splitting of the Fe-As in-plane phonon and the phonon energies from both surfaces are consistent for the whole temperature range. The splitting energy scales linearly with the in-plane lattice order parameter of the structural phase transition. However, while our measurements of the strain-free sample indicate that the C_4 symmetry breaking occurs only at T_S upon cooling, our results show that the strain field induced by cutting samples with a razor blade breaks the C_4 symmetry above T_S, which may provide an explanation for the observed anisotropy above T_S in various measurements of samples under uniaxial strain.

[1] G. R. Stewart, Rev. Mod. Phys. **83**, 1589 (2011).

[2] I. R. Fisher, L. Degiorgi, and Z. X. Shen, Rep. Prog. Phys. **74**, 124506 (2011).

[3] T. Terashima, N. Kurita, M. Tomita, K. Kihou, C.-H. Lee, Y. Tomioka, T. Ito, A. Iyo, H. Eisaki, T. Liang, M. Nakajima, S. Ishida, S.-i. Uchida, H. Harima, and S. Uji, Phys. Rev. Lett. **107**, 176402 (2011).

[4] M. Nakajima, S. Ishida, Y. Tomioka, K. Kihou, C. H. Lee, A. Iyo, T. Ito, T. Kakeshita, H. Eisaki, and S. Uchida, Phys. Rev. Lett. **109**, 217003 (2012).

[5] X. Lu, J. T. Park, R. Zhang, H. Luo, A. H. Nevidomskyy, Q. Si, and P. Dai, Science **345**, 657 (2014).

[6] J.-H. Chu, J. G. Analytis, K. De Greve, P. L. McMahon, Z. Islam, Y. Yamamoto, and I. R. Fisher, Science **329**, 824 (2010).

[7] M. Yi, D. Lu, J.-H. Chu, J. G. Analytis, A. P. Sorini, A. F. Kemper, B. Moritz, S.-K. Mo, R. G. Moore, M. Hashimoto, W.-S. Lee, Z. Hussain, T. P. Devereaux, I. R. Fisher, and Z.-X. Shen, Proc. Natl. Acad. Sci. USA **108**, 6878 (2011).

[8] E. Thewalt, J. P. Hinton, I. M. Hayes, T. Helm, D. H. Lee, J. G. Analytis, and J. Orenstein, arXiv:1507.03981.

[9] S. Kasahara, H. Shi, K. Hashimoto, S. Tonegawa, Y. Mizukami, T. Shibauchi, K. Sugimoto, T. Fukuda, T. Terashima, A. H. Nevidomskyy *et al.*, Nature (London) **486**, 382 (2012).

[10] F. L. Ning, K. Ahilan, T. Imai, A. S. Sefat, M. A. McGuire, B. C. Sales, D. Mandrus, P. Cheng, B. Shen, and H.-H. Wen, Phys. Rev. Lett. **104**, 037001 (2010).

[11] M. Yoshizawa, D. Kimura, T. Chiba, S. Simayi, Y. Nakanishi, K. Kihou, C.-H. Lee, A. Iyo, H. Eisaki, M. Nakajima, and S.-i. Uchida, J. Phys. Soc. Jpn. **81**, 024604 (2012).

[12] T. Goto, R. Kurihara, K. Araki, K. Mitsumoto, M. Akatsu, Y. Nemoto, S. Tatematsu, and M. Sato, J. Phys. Soc. Jpn. **80**, 073702 (2011).

[13] A. E. Böhmer, P. Burger, F. Hardy, T. Wolf, P. Schweiss, R. Fromknecht, M. Reinecker, W. Schranz, and C. Meingast, Phys. Rev. Lett. **112**, 047001 (2014).

[14] Y. Gallais, R. M. Fernandes, I. Paul, L. Chauvière, Y.-X. Yang, M.-A. Méasson, M. Cazayous, A. Sacuto, D. Colson, and A. Forget, Phys. Rev. Lett. **111**, 267001 (2013).

[15] Y.-X. Yang, Y. Gallais, R. M. Fernandes, I. Paul, L. Chauvière, M.-A. Méasson, M. Cazayous, A. Sacuto, D. Colson, and A. Forget, JPS Conf. Proc. **3**, 015001 (2014).

[16] F. Kretzschmar, T. Böhm, U. Karahasanović, B. Muschler, A. Baum, D. Jost, J. Schmalian, S. Caprara, M. Grilli, C. Di Castro, J. G. Analytis, J.-H. Chu, I. R. Fisher, and R. Hackl, arXiv:1507.06116.

[17] V. K. Thorsmølle, M. Khodas, Z. P. Yin, C. Zhang, S. V. Carr, P. Dai, and G. Blumberg, Phys. Rev. B **93**, 054515 (2016).

[18] W.-L. Zhang, P. Richard, H. Ding, A. S. Sefat, J. Gillett, S. E. Sebastian, M. Khodas, and G. Blumberg, arXiv:1410.6452.

[19] P. Massat, D. Farina, I. Paul, S. Karlsson, P. Strobel, P. Toulemonde, M.-A. Measson, M. Cazayous, A. Sacuto, S. Kasahara, T. Shibauchi, Y. Matsuda, and Y. Gallais, arXiv:1603.01492.

[20] C. Dhital, Z. Yamani, W. Tian, J. Zeretsky, A. S. Sefat, Z. Wang, R. J. Birgeneau, and S. D. Wilson, Phys. Rev. Lett. **108**, 087001 (2012).

[21] S. D. Wilson, Z. Yamani, C. R. Rotundu, B. Freelon, E. Bourret-Courchesne, and R. J. Birgeneau, Phys. Rev. B **79**, 184519 (2009).

[22] X. Ren, L. Duan, Y. Hu, J. Li, R. Zhang, H. Luo, P. Dai, and Y. Li, Phys. Rev. Lett. **115**, 197002 (2015).

[23] A. S. Sefat, R. Jin, M. A. McGuire, B. C. Sales, D. J. Singh, and D. Mandrus, Phys. Rev. Lett. **101**, 117004 (2008).

[24] M. A. Tanatar, A. Kreyssig, S. Nandi, N. Ni, S. L. Bud'ko, P. C. Canfield, A. I. Goldman, and R. Prozorov, Phys. Rev. B **79**, 180508 (2009).

[25] A. P. Litvinchuk, V. G. Hadjiev, M. N. Iliev, B. Lv, A. M. Guloy, and C. W. Chu, Phys. Rev. B **78**, 060503 (2008).

[26] E. Kroumova, M. Aroyo, J. Perez-Mato, A. Kirov, C. Capillas, S. Ivantchev, and H. Wondratschek, Phase Transit. **76**, 155 (2003).

[27] M. Zbiri, H. Schober, M. R. Johnson, S. Rols, R. Mittal, Y. Su, M. Rotter, and D. Johrendt, Phys. Rev. B **79**, 064511 (2009).

[28] L. Chauvière, Y. Gallais, M. Cazayous, A. Sacuto, M. A. Méasson, D. Colson, and A. Forget, Phys. Rev. B **80**, 094504 (2009).

[29] M. Tegel, M. Rotter, V. Wei, F. M. Schappacher, R. Pttgen, and D. Johrendt, J. Phys.: Condens. Matter **20**, 452201 (2008).

[30] J. Menéndez and M. Cardona, Phys. Rev. B **29**, 2051 (1984).

[31] X. Chen, L. Harriger, A. Sefat, R. J. Birgeneau, and S. D. Wilson, Phys. Rev. B **93**, 144118 (2016).